Journal of Molecular Structure 1076 (2014) 730–736

Contents lists available at ScienceDirect

Journal of Molecular Structure

journal homepage: www.elsevier.com/locate/molstruc

Synthesis, crystal structure, spectroscopic properties, DFT calculation and biological activity of 4-chloro-N-(2-(2-nitrophenyl)acetoxy)-N-phenylbenzamide

Dian He [a,b,*], Zhu-Qing Yang [a], Meng Hou [a], Chong Teng [c], Xiao-Hong Wang [b]

[a] Institute of Medicinal Chemistry, School of Pharmaceutical Science, Lanzhou University, Lanzhou 730000, PR China
[b] State Key Laboratory of Applied Organic Chemistry, Lanzhou University, Lanzhou 730000, PR China
[c] Faculty of Science, Beijing University of Chemical Technology, Beijing 100029, PR China

HIGHLIGHTS

- 4-Chloro-N-(2-(2-nitrophenyl)acetoxy)-N-phenylbenzamide was synthesized.
- Its structure was characterized by NMR, MS, IR, X-ray and cyclic voltammetry.
- Some molecular properties were calculated by density functional theory calculations.
- Antitumor potencies were evaluated in vitro.

GRAPHICAL ABSTRACT

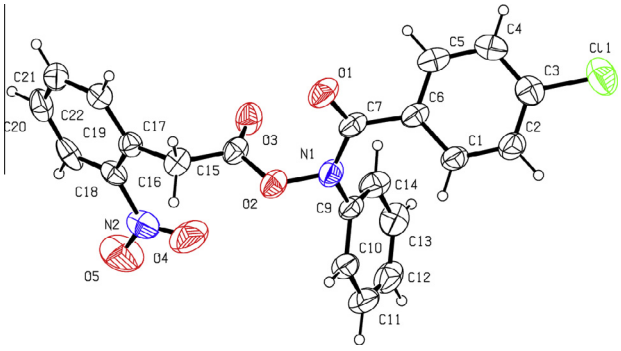

ARTICLE INFO

Article history:
Received 10 June 2014
Received in revised form 20 August 2014
Accepted 20 August 2014
Available online 28 August 2014

Keywords:
N-phenylbenzamide
Crystal structure
Cyclic voltammetry
DFT
Antitumor activity

ABSTRACT

4-Chloro-N-(2-(2-nitrophenyl)acetoxy)-N-phenylbenzamide was synthesized and characterized by ^{1}H NMR, ^{13}C NMR, MS, IR and X-ray diffraction methods. The structure–property relationship and the antitumor activity based on electrochemical measurements, density functional theory calculations (DFT) and methylthiazolyldiphenyl-tetrazolium bromide (MTT) assay were investigated. The crystal structure adopts monoclinic space group *P21/n* with the unit cell parameters of $a = 12.4385(10)$ Å, $b = 6.5036(5)$ Å, $c = 24.7944(19)$ Å, $\beta = 103.045(9)°$, $V = 1954.0(3)$ Å^3, $Z = 4$, and stabilized by π–π conjugation and hydrogen bonding interactions. The observed results of the compound have been compared with theoretical results and it is found that the experimental data show good agreement with calculated values. And the compound had slightly better inhibition than suberoylanilide hydroxamic acid (SAHA) in NCI-H460 cell line as well as the nearly same as SAHA in MCF-7, HCT-116, PC-3, and A549 cell lines.

Introduction

The compound containing hydroxamic acid analogues has been paid intensively attention due to the diverse biological properties. In particular, phenyl hydroxamic acid derivatives as histone deacetylase (HDAC) play a key role to inhibit tumor growth [1–3]. Special hydroxamic acid structural fragment can build the complexation with Zn^{2+} in the bottom of HDAC, such as NVP2LAQ824, pyroxamide, oxamflatin, and scriptaid [4], which can affect acetylation level of histone, change the structure and the function of chromatin, and regulate expression level of gene. However, hydroxamic acid with strong carcinogenicity has strong inhibition

* Corresponding author at: Institute of Medicinal Chemistry, School of Pharmaceutical Science, Lanzhou University, Lanzhou 730000, PR China. Tel.: +86 13008738922.
E-mail address: hed@lzu.edu.cn (D. He).

http://dx.doi.org/10.1016/j.molstruc.2014.08.042
0022-2860/

against the normal human cell [2]. Thus we link *o*-nitrophenylacetic acid as the carrier with hydroxamic acid. These derivatives are easier reduced and hydrolyzed in tumor cells than normal cells because of the low pH value, the highly active reductase and hydrolase [5], which can lead to the rapid reduction of nitro and hydrolysis of ester. Then *o*-nitrophenylacetic acid may cyclize to form a stable six-membered ring and release benzohydroxamic acid with antitumor activity. So the conjugation of *o*-nitrophenylacetic acid and hydroxamic acid which is easier synthesized increases the selectivity to tumor cell. Meanwhile, the conjugation not undergoing nitro reduction may also occur hydrolysis with associated hydrolase, and then release hydroxamic acid.

Here, with reference to the prospect of the potent biological effect and the high selectivity to tumor cell resulting in the low toxicity, 4-chloro-N-(2-(2-nitrophenyl)acetoxy)-N-phenylbenzamide was synthesized, and its single crystal X-ray diffraction analysis, spectroscopic and electrochemical measurements, properties, density functional theory calculations, and in vitro biological activity assay were carried out.

Experiment

Materials and measurements

Nitrobenzene, 4-chlorobenzoyl chloride, and 2-nitrophenylacetic acid were purchased from j&k (China). The melting point determination was performed on electrothermal PIF YRT-3 apparatus without thermometer rectification. Infrared spectra were recorded with a Perkin-Elmer Spectrum 2000 FTIR spectrometer in KBr pellets. ^{1}H NMR and ^{13}C NMR (δ ppm) spectra were recorded ($CDCl_3$ solution) on a Varian Mercury (400 MHz) using TMS as the internal standard. Mass spectra were recorded on a VGZAB-HS (70 eV) spectrometer with ESI source as ionization.

Preparation of N-(4-chlorophenyl)-N-(2-(2-nitrophenoxy)acetoxy)benzamide

Acylation reaction of 4-chlorobenzoyl chloride and the reductive matter of nitrobenzene gave compound (**1**) [6,7]. Compound (**2**) (10 mmol) was slowly dropwise poured into the solution of compound (**1**) (10 mmol) in 30 mL dichloromethane. The mixture was stirred for 1.5 h and monitored by thin layer chromatography (TLC). After filtration, the solution was concentrated under reduced pressure, and then recrystallization from methanol gave the white powder (Scheme 1). The colorless crystal of title compound suitable for X-ray structure analysis was obtained from dichloromethane–ethanol (*v*/*v*, 1:3) with slow evaporation at room temperature. Yield 85%, m.p.: 120–121 °C. IR (KBr) ν (cm^{-1}): 3433 (—N—C=O), 1780 (—C=O), 1526 (—NO_2), 1348 (—NO_2), 1077 (N—O), 863 (C—N); ^{1}H NMR (400 MHz, $CDCl_3$) δ: 8.14 (d, J = 7.6 Hz, 1H), 7.63 (d, J = 6.4 Hz, 1H), 7.62 (d, J = 6.4 Hz, 1H), 7.50 (t, J = 7.6 Hz, 2H), 7.47 (d, J = 6.0 Hz, 1H), 7.44 (d, J = 8.4 Hz, 1H), 7.34 (d, J = 8.0 Hz, 1H), 7.30 (t, J = 7.2 Hz, 2H), 7.26 (d, J = 6.4 Hz, 1H), 7.23 (d, J = 8.8 Hz, 1H), 4.18 (s, 2H, —CH_2); ^{13}C NMR (100 MHz, $CDCl_3$) δ: 167.6, 165.6, 148.2, 140.0, 137.4, 137.4, 133.9, 133.5, 131.3, 131.3, 130.3, 129.3, 129.1, 129.1, 128.8, 128.4, 128.1, 128.1, 126.9, 125.4, 37.3. HRMS (ESI): (M + NH_4^+) 428.1008 (calculated 428.8427), error = 2.3 ppm.

Determination of the crystal structure

A colorless crystal of the title compound with dimensions of 0.37 mm × 0.35 mm × 0.25 mm was selected for X-ray diffraction analysis. The data collection was performed at 293 K on SuperNova, Dual, Cu at zero, Eos diffractometer with Mo Kα radiation (λ = 0.71073 Å) [8,9]. The structure was solved by direct methods with SHELX.97 [10] and refined by SHELXL.97 [11]. All non-hydrogen atoms were refined with anisotropic thermal parameters. The hydrogen atoms were placed in the calculated positions.

Electrochemistry

Cyclic voltammetry (CV) was performed with a CHI 600 electrochemical workstation (Shanghai Shenhua Instrument Co., Ltd. Shanghai, China) in a conventional three-electrode electrochemical cell using glassy carbon as the working electrode, a saturated calomel electrode as reference electrode, and a Pt slice electrode as auxiliary electrode. The target compound solution containing 0.10 mol/L KCl at the concentration of 6.0×10^{-3} mol/L was prepared with pH 6.5 phosphate buffer. The cyclic voltammetry investigation was performed by sweeping the potential between −1.9 V and +1 V (vs. Ag/AgCl) for one cycle at the scan rate of 100 mV/s to record the reduction potential. The oxygen of all solutions was removed by purging high-purity nitrogen.

In vitro cytotoxicity assay

The proliferation inhibition assay of the title compound was tested in MCF-7, HCT-116, PC-3, A549, NCI-H460 cell lines, which were maintained at 37 °C in 5% CO_2 in dulbecco's modification of eagle's medium dulbecco (DMEM), supplemented with 10% fetal calf serum. Exponentially growing cells, representing an asynchronous population, were seeded in 96-well plates, at the density of 5000–10,000 cells per well while the marginal wells should be

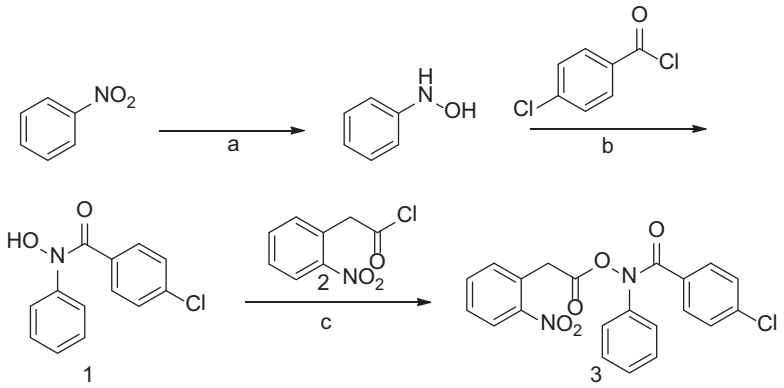

Scheme 1. Synthetic route of 4-chloro-N-(2-(2-nitrophenyl)acetoxy)-N-phenylbenzamide. Reagents and conditions: (a) NH2NH2·H2O, Raney nickel, CH3CH2OH/ClCH2CH2Cl (3:2), 0 °C; (b) tetrahydrofuran, NaHCO3, 0 °C; (c) CH2Cl2, NaHCO3, rt.

omitted. The cells were allowed to stabilize on plates by incubating for 24 h. One hundred microlitres of the corresponding concentration compounds were added into the wells in triplicate, while equivalent amount of medium was added to the control wells. The cells were mixed gently and incubated further for 48 h. Then 10 μL of MTT stock solution (5 mg/mL in PBS) was added in each well and the plate was incubated for 4 h. The formed blue-colored formazan was dissolved in 100 μL of DMSO per well. After mixed for 10 min, the absorbance was determined at 490 nm to calculate the half maximal (50%) inhibitory concentration (IC) of a substance (IC_{50}). IC_{50} (μM) was defined as the amount of cytotoxicity causing an inhibition of 50% in the viability of the cells compared with the control cell culture.

Results and discussions

Crystal structure

The crystal data, collected reflections, and parameters of the final refinement are reported in Table 1. The single crystal structure is shown in Fig. 1. This dimers stabilize crystal packing in three dimensional space as shown in Fig. 2.

The values of the selected bond lengths and bond angles were dramatically in accordance with their calculated counterparts as

Table 1
Crystallographic data and structure refinement parameters of the title compound.

Empirical formula	C_{21} H_{15} Cl N_2 O_5
Formula weight	410.80
Temperature (*K*)	293 K
Crystal system	Monoclinic
Space group	P21/n
a/Å	12.4385(10)
b/Å	6.5036(5)
c/Å	24.7944(19)
α/°	90.00
β/°	103.045(9)
γ/°	90.00
Volume/Å^3	1954.0(3)
Z	4
ρ_{calc} mg/mm^3	1.396
μ (Mo Kα) (mm^{-1})	0.231
F (000)	848.0
Crystal size (mm^3)	0.37 × 0.35 × 0.25
Index ranges	$-15 \leqslant h \leqslant 14$, $-7 \leqslant k \leqslant 8$, $-30 \leqslant l \leqslant 30$
Radiation	Mo Kα (λ = 0.7107)
Reflections collected	7379
Independent reflections	3838
Radiation	Mo Kα (λ = 0.7107)
Final *R* indices [$I > 2\sigma(I)$]	R_1 = 0.0581, wR_2 = 0.1440
Final *R* indexes [all data]	R_1 = 0.1029, wR_2 = 0.1822
Largest diff. peak/hole/e Å^{-3}	0.21/−0.24
Goodness-of-fit on F^2	1.031
CCDC deposit number	995,288

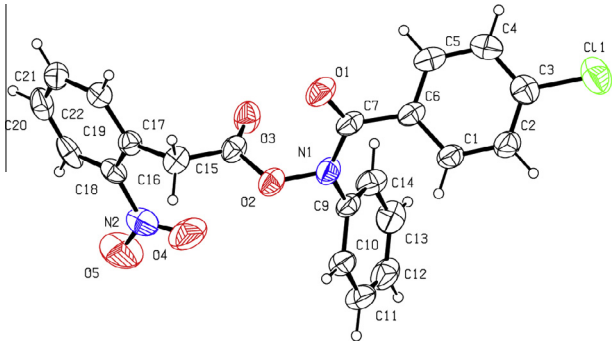

Fig. 1. Atom numbering scheme for the target compound.

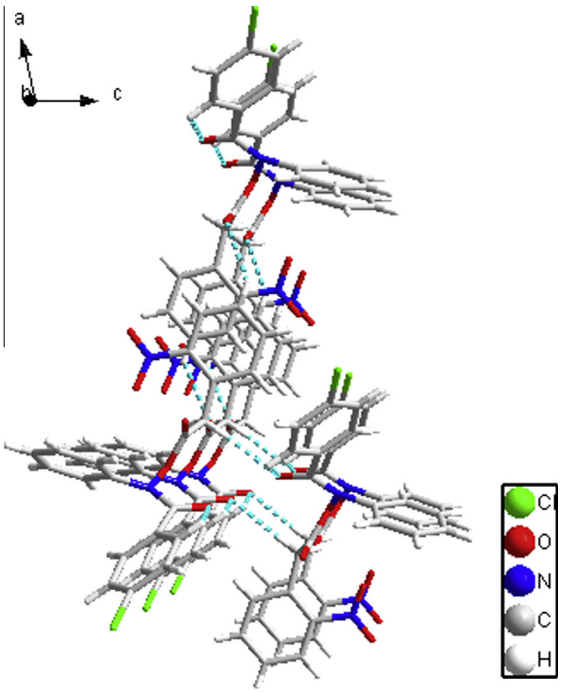

Fig. 2. Packing diagram of the target compound.

are summarized in Table 2. The crystal structure is not coplanar according to the torsion angle C5—C6—C7—O1(−38.7°) and C1—C6—C7—O1(134.8°). In the nitro-substituted benzene ring (C(17)—C(22)), the dihedral angle between chloro-phenyl ring (C(1)—C(6)) and benzene ring (C(9)—C(14)) plane is 25.91(44)°. C(7)—N(1) bond (1.36 Å) is shorter than regular C—N bond (1.47 Å), but longer than C═N double bond (1.323 Å) due to P–π conjugation effect. The sum of O(1)—C(7)—N(1), O(1)—C(7)—C(6), and N(1)—C(7)—C(6) angles are 360°, which indicates sp^2 hybridization state of the C(9) atom (Table 2). Furthermore, two Cg2 ring of adjacent molecules are parallel and the distance of them is 4.75 Å, as shows the presence of π–π stacking in the packing (Table 3). The crystal structure also exhibits intra/intermolecular hydrogen bonding interactions (Table 4), together with π–π conjugation stabilize the compound structure, and the distances between donors and acceptors for all hydrogen bonds are in the range of 3.302–3.451 Å. For example, atom C20 of nitro-substituted benzene ring at (17,907, 14,822, 2976.8) as hydrogen bond donor and atom O3 of ester ring at (14500.0, 11,122, 1956.9) as hydrogen bond acceptor form the intermolecular hydrogen bond C(20)—H(20)···O(3) via atom H20, and the distance between C(20) and O(3) is 3.302 Å.

^{1}H NMR spectrum and IR spectrum

^{1}H NMR spectra was measured with a Varian unity INOVA-400 nuclear magnetic resonance and the chemical shifts were expressed in ppm relatively to TMS. The DFT/B3LYP methods with the 6-311G+(d, p) basis set was also used to calculate the chemical shifts. The results of the experimental and calculated value with respect to TMS are shown in Table 5. The chemical shifts of aromatic protons of organic molecules are usually observed in the range of 7.00–8.00 ppm and the theoretical H chemical shift are all nearly in agreement with the experimental observations except the active hydrogen with mean absolute deviation 1.8 ppm. The experimental values of the target compound were reported at 7.23–8.14 ppm in $CDCl_3$ solvent, the calculated ones at 7.21–8.34 ppm for B3LYP level. The chemical shift, 8.14 ppm of H

Table 2
Selected geometrical parameters of the title compound with X-ray structure and DFT methods.

	Exp.	B3LYP 6-311G(d, p)		Exp.	B3LYP 6-311G(d, p)
Bond lengths (Å)			Bond lengths (Å)		
Cl1—C3	1.733(4)	1.756(3)	C6—C7	1.487(4)	1.501(2)
O1—C7	1.221(3)	1.217	C9—C10	1.387(4)	1.397
O2—N1	1.419(3)	1.412	C9—C14	1.364(5)	1.398
O2—C15	1.389(3)	1.391	C10—C11	1.373(5)	1.392
O3—C15	1.181(4)	1.191	C11—C12	1.368(6)	1.393
O4—N2	1.212(4)	1.227	C12—C13	1.367(5)	1.369
O5—N2	1.207(3)	1.221	C13—C14	1.379(4)	1.391
N1—C7	1.362(4)	1.391	C15—C16	1.494(4)	1.521
N1—C9	1.428(3)	1.429	C16—C17	1.501(4)	1.514
N2—C18	1.459(4)	1.486	C17—C18	1.389(4)	1.406
C1—C2	1.380(4)	1.392	C17—C22	1.389(4)	1.391
C1—C6	1.385(4)	1.400	C18—C19	1.393(4)	1.395
C2—C3	1.378(4)	1.390	C19—C20	1.368(4)	1.387
C3—C4	1.371(5)	1.378	C20—C21	1.356(5)	1.392
C4—C5	1.383(5)	1.388	C21—C22	1.367(4)	1.390
C5—C6	1.385(4)	1.401			
Bond angles (°)			Bond angles (°)		
C15—O2—N1	112.8(2)	113.9	C14—C9—N1	121.3(3)	118.2
O2—N1—C9	113.5(2)	113.3	C14—C9—C10	120.8(3)	121.4
C7—N1—O2	114.3(2)	119.8	C11—C10—C9	118.9(4)	119.3
C7—N1—C9	130.9(3)	131.3	C12—C11—C10	120.2(4)	120.8
O4—N2—C18	119.8(3)	119.8	C13—C12—C11	120.6(4)	120.9
O5—N2—O4	121.6(4)	121.5	C12—C13—C14	119.8(4)	118.9
O5—N2—C18	118.6(4)	117.3	C9—C14—C13	119.6(3)	119.8
C2—C1—C6	120.2(3)	120.6	O2—C15—C16	108.1(3)	108.5
C3—C2—C1	119.9(3)	119.3	O3—C15—O2	123.6(3)	123.3
C2—C3—Cl1	118.9(3)	119.5	O3—C15—C16	128.3(3)	127.6
C4—C3—Cl1	120.4(3)	121.1	C15—C16—C17	113.6(2)	112.6
C4—C3—C2	120.8(3)	120.5	C18—C17—C16	126.4(3)	125.8
C3—C4—C5	119.2(3)	119.6	C18—C17—C22	115.6(3)	114.8
C4—C5—C6	120.9(3)	121.0	C22—C17—C16	118.0(2)	118.6
C1—C6—C5	119.0(3)	119.4	C17—C18—C19	122.1(3)	122.0
C1—C6—C7	122.7(3)	125.4	C19—C18—N2	117.2(3)	115.6
C5—C6—C7	118.0(3)	115.4	C20—C19—C18	119.1(3)	120.0
O1—C7—N1	121.3(3)	119.5	C21—C20—C19	120.3(3)	119.4
O1—C7—C6	121.4(3)	120.9	C20—C21—C22	120.1(3)	120.0
N1—C7—C6	117.2(3)	119.6	C21—C22—C17	122.7(3)	122.3
C10—C9—N1	117.9(3)	121.6	C17—C18—N2	120.7(3)	120.5
Torsion angle (°)			Torsion angle (°)		
Cl1—C3—C4—C5	179.9(2)	119.3	C5—C6—C7—N1	145.1(3)	−34.22
O2—N1—C7—O1	−5.1(4)	−5.5	C6—C1—C2—C3	0.3(5)	0.023
O2—N1—C7—C6	171.1(2)	171.0	C7—N1—C9—C10	140.7(3)	139.7
O2—N1—C9—C10	−53.4(3)	−55.9	C7—N1—C9—C14	−40.3(4)	−41.2
O2—N1—C9—C14	125.5(3)	124.6	C9—N1—C7—O1	160.7(3)	162.3
O2—C15—C16—C17	−161.0(2)	−143.1	C9—N1—C7—C6	−23.1(4)	−19.8
O3—C15—C16—C17	20.9(4)	21.2	C9—C10—C11—C12	1.5(5)	0.9
O4—N2—C18—C17	−14.7(5)	−15.4	C10—C9—C14—C13	−1.7(4)	−1.3
O4—N2—C18—C19	164.9(3)	165.7	C10—C11—C12—C13	−1.4(6)	−0.9
O5—N2—C18—C17	167.0(3)	158.4	C11—C12—C13—C14	−0.3(5)	−0.2
O5—N2—C18—C19	−13.4(4)	−21.6	C12—C13—C14—C9	1.8(5)	2.1
N1—O2—C15—O3	3.4(4)	3.6	C14—C9—C10—C11	0.1(4)	0.4
N1—O2—C15—C16	−174.9(2)	−170.1	C15—O2—N1—C7	78.2(3)	69.9
N1—C9—C10—C11	179.1(3)	179.8	C15—O2—N1—C9	−90.1(3)	−89.5
N1—C9—C14—C13	179.3(3)	178.9	C15—C16—C17—C18	74.8(4)	91.4
N2—C18—C19—C20	−179.1(3)	122.9	C15—C16—C17—C22	−106.3(3)	−121.5
C1—C2—C3—Cl1	−179.9(2)	119.3	C16—C17—C18—N2	−1.1(4)	−2.2
C1—C2—C3—C4	−0.2(5)	−0.1	C16—C17—C18—C19	179.3(3)	179.5
C1—C6—C7—O1	134.8(3)	129.8	C16—C17—C22—C21	−179.6(3)	−179.8
C1—C6—C7—N1	−41.4(4)	−34.2	C17—C18—C19—C20	0.5(4)	0.1
C2—C1—C6—C5	−0.4(4)	−0.3	C18—C17—C22—C21	−0.6(5)	−0.5
C2—C1—C6—C7	−173.8(3)	−172.5	C18—C19—C20—C21	−1.3(5)	−0.72
C2—C3—C4—C5	0.3(5)	0.5	C19—C20—C21—C22	1.1(5)	0.4
C3—C4—C5—C6	−0.4(5)	−0.3	C20—C21—C22—C17	−0.2(5)	−0.5
C4—C5—C6—C1	0.4(4)	0.2	C22—C17—C18—N2	180.0(3)	179.9
C4—C5—C6—C7	174.2(3)	176.4	C22—C17—C18—C19	0.4(4)	0.3
C5—C6—C7—O1	−38.7(4)	−39.9			

(14C Ar—H) is apparently higher than the regular value, which may result from electronic effect of carbonyl (7C) closer in space. Furthermore, the O1 of carbonyl (7C) as the acceptor can form a intermolecular hydrogen bond via H16 with the donor C16. The carbonyl (15C) has strong deshielding effect to H16, which can move the resonance of nearby proton towards to a higher frequency. Hence, the chemical shift of H16 at the 4.71 ppm is much higher the normal value (1.00 ppm) based on above two effects.

To gain furthermore information on the crystal structure, we have undertaken a vibrational study using infrared spectroscopy

Table 3
π–π Stacking interactions (Å, °).

Cg(I) Res(I) Cg(J)	[ARU(J)]	Cg–Cg	Alpha	CgI_Perp	CgJ_Perp	Slippage
Cg(2) [1] → Cg(2)	[3655.01]	4.7548	0	3.3943	3.3943	3.330
Cg(3) [1] → Cg(3)	[2645.01]	3.8443	1	3.2560	−3.2473	
Cg(3) [1] → Cg(3)	[2655.01]	3.8443	1	−3.2473	3.2560	

Symmetry codes: [3655] = 1−*X*, −*Y*, −*Z*; [2645] = 3/2−*X*, −1/2 + *Y*, 1/2−*Z*; [2655] = 3/2−*X*, 1/2 + *Y*, 1/2−*Z*.

Table 4
Geometry of proposed C—H···O close contacts.

D—H···A	d(D—H)	d(H···A)	d(D···A)	<DHA
C(5)—H(5)···O(1)[i]	0.93	2.54	3.451	167
C(16)—H(16A)···O(1)[ii]	0.97	2.37	3.338	174
C(20)—H(20)···O(3)[iii]	0.93	2.57	3.302	136

Symmetry codes:
[i] 1/2−*x*, −1/2 + *y*, 1/2−*z*.
[ii] 1/2−*x*, 1/2 + *y*, 1/2−*z*.
[iii] 3/2−*x*, 1/2 + *y*, 1/2−*z*.

Table 5
Theoretical and experimental ^{1}H NMR (all values in ppm) for the target compound.

Proton	Experimental	B3LYP/6-311g+(d, p)	
		σ(^{1}H)	|A.D.|
1H(1C Ar—H)	7.47	7.90	0.43
1H(2C Ar—H)	7.30	7.45	0.15
1H(4C Ar—H)	7.27	7.22	0.05
1H(5C Ar—H)	7.43	7.90	0.47
1H(10C Ar—H)	7.63	7.53	0.10
1H(11C Ar—H)	7.52	7.45	0.07
1H(12C Ar—H)	7.48	7.21	0.27
1H(13C Ar—H)	7.52	7.45	0.07
1H(14C Ar—H)	8.14	8.34	0.02
2H(16C CH_2)	4.71	5.68	1.97
		2.91	1.80
1H(19C Ar—H)	7.63	8.16	0.53
1H(20C Ar—H)	7.32	7.45	0.13
1H(21C Ar—H)	7.30	7.33	0.03
1H(22C Ar—H)	7.23	7.22	0.01

A.D. refers to the absolute deviation.

as the related vibrational spectra data are listed in Table 6. The characteristic *v* (CH) stretching vibrations of aromatic structures are expected to appear in 3000–3100 cm^{-1} region. In the present study, *v* (CH) symmetric and asymmetric stretching modes are observed at 3038 cm^{-1}, 3067 cm^{-1} respectively. The bands at 2926 cm^{-1} and 2849 cm^{-1} indicated the presence of aliphatic methylene. There are two strong signals at 1791 cm^{-1} and 1664 cm^{-1} showing the presence of carbonyl functional group while the regular carbonyl vibration frequency is generally observed at 1715 cm^{-1}. Carbonyl O1 as the acceptor of amide in molecular structure can form an intermolecular hydrogen bond via H16 with C16 as the donor in the adjacent molecules, which will decrease its vibration frequency. Hence, the band at 1664 cm^{-1} can be assigned the carbonyl of amide. The experimental and theoretical value of NO_2 stretching vibrations are reported at 1524 cm^{-1}, 1348 cm^{-1} and 1522 cm^{-1}, 1345 cm^{-1} respectively. Also, the signals in the range of 716–993 cm^{-1} are attributed to Ar—H bending vibration. Despite the differences between observed and calculated values, the general agreement is good.

Cyclic voltammetry

The determination of reduction potential for the title compound ($c = 6.0 \times 10^{-3}$ mol/L) was carried out with the cyclic voltammetry

Table 6
Vibrational frequencies of the title compound with experimental and DFT/B3LYP methods.

Frequencies	Experimental	B3LYP/6-311g+(d, p)	
		Value	|A.D.|
v(N—C=O)	3426	3428	2
$v_{as}(CH_2)$all	2926	2924	2
v_s(CH)phe	3067	3068	1
$v_{as}(CH_2)$phe	3038	3036	2
v_s(CH)all	2849	2852	3
v(C=C)phe	1522–1664	1524–1660	2–4
v(O=C—C)	1791	1796	5
v(O=C—N)	1664	1668	4
$v_s(NO_2)$	1522	1524	2
$v_{as}(NO_2)$	1345	1348	3
δ(CH)all	1455	1452	3
δ(CH)phe	716–993	716–996	0–3

all.: allyl, phe.: phenyl, *v*: stretching, v_{as}: asymmetric stretching, v_s: symmetric stretching, δ: bending.
A.D. refers to the absolute deviation.

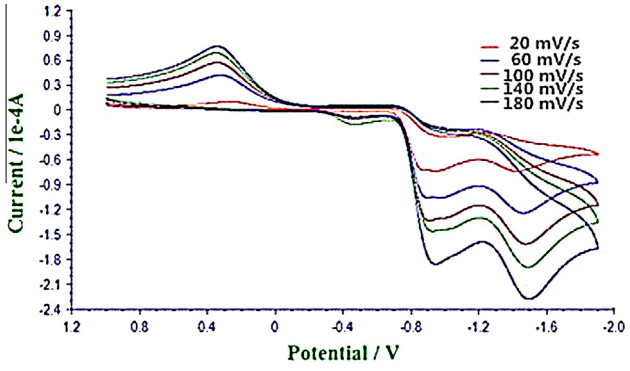

Fig. 3. Cyclic voltammetry of the title compound at different scan rates in methanol.

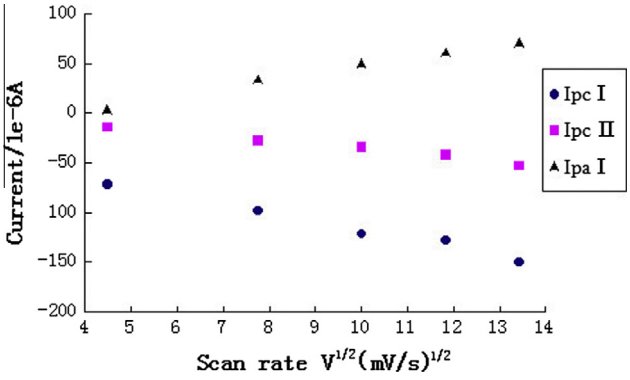

Fig. 4. Anodic and cathodic peak current (i_{pa}/i_{pc}) of the title compound at different scan rates in methanol.

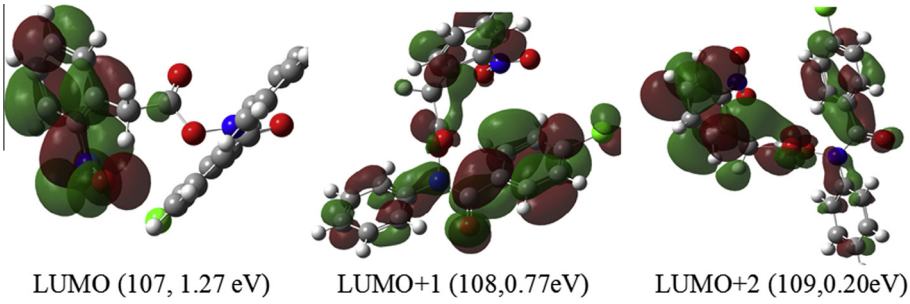

Fig. 5. Energy diagram of the first three LUMOs of the target compound.

technique in methanol containing KCl (c = 0.10 mol/L) as a supporting electrolyte by sweeping the potential between −1.9 V and +1 V (vs. Ag/AgCl) at a scan rate of 100 mV/s.

Two reductive peaks and one oxidative peak are shown in the cyclic voltammetry curve (Fig. 3), which are all not electrochemically equivalent. According to the literature [12,13], the peak from −0.6 V to −1.1 V is produced in the reduction from nitro to hydroxylamine. But as is well known, hydroxylamine as an unstable intermediate would be further reduced to amino. It may be resulted in another reduction potential peak appearing between −1.3 V and −1.5 V. Hence, the reduction from nitro to hydroxylamine, then to amino leads to a −0.907 V peak of the first reduction and a −1.479 V peak of the subsequent one.

Fig. 3 also shows the redox peak currents increase simultaneously without the significant change of peak potential along with the increase of scan rate over the range of 20–180 mV/s, which is mainly reasoned for the internal resistance of the electrode. Both the anodic and cathodic peak currents are linear to the square root of scan rates ($v^{1/2}$) (Fig. 4), indicating that the redox process was mainly controlled by diffusion and conducted on the electrode surface [14].

Theoretical calculation

The structure of the title compound optimized by DFT is in congruent with the actual crystal structure, which some frontier molecular orbitals are shown in Fig. 5. The lowest unoccupied molecular orbital (LUMO) thought the innermost orbital containing free places to accept electrons have been calculated. LUMO + 1 (0.77 eV), LUMO + 2 (0.20 eV), and LUMO (1.27 eV) are seem to be π-bonding type orbitals, among which the electron clouds of LUMO + 1 (0.77 eV) and LUMO + 2 (0.20 eV) are nearly delocalized all over molecule, and LUMO (1.27 eV) is mainly dominated by the nitro-substituted benzene ring.

In vitro tumor proliferation inhibition of the target compound

The title compound with SAHA as the positive control was tested in the proliferation inhibition assay in MCF-7, HCT-116, PC-3, A549, and NCI-H460 cell lines as are described in Table 7. It is in agreement with literature [15,16] and the National Cancer Institute-Development Therapeutic Program (NCI-DTP) data for SAHA. As expected, the title compound with the IC_{50} values of 4.07 μM, 7.36 μM, 6.53 μM, and 4.85 μM, respectively, in MCF-7, HCT-116, PC-3, and A549 cell lines, has good proliferation inhibition, which is equivalent to SAHA. But in NCI-H460 cell line, the proliferation inhibition (IC_{50} = 1.76 μM) of the target compound is slightly better than the one (IC_{50} = 2.92 μM) of SAHA, which may be owing to good membrane permeability resulting from the absence of the highly polar character of hydroxamic acid for the title compound because of induction of *o*-nitrophenylacetic acid into the target compound [15]. Hence, the designed and synthesized hydroxamic acid derivative is expected to be developed as a novel antitumor agent, and the further study is underway to investigate the selectivity to tumor cell.

Table 7
Cytotoxicity of the target compound (IC_{50}, μM).

	MCF-7[a]	HCT-116[a]	PC-3[a]	A549[a]	NCI-H460[a]
The title compound	4.07	7.36	6.53	4.85	1.76
SAHA	5.65	6.21	5.02	5.36	2.92

[a] Values are the mean of three separate experiments.

Conclusion

In this paper, 4-chloro-N-(2-(2-nitrophenyl)acetoxy)-N-phenylbenzamide was synthesized and characterized by spectroscopic (^{1}H NMR, ^{13}C NMR, MS, IR) and single crystal X-ray diffraction, of which most of the structural properties were calculated by using B3LYP/6-311G (d, p) basis sets, and antitumor activity was proceeded in the five cancer cell lines. It was resulted in that hydrogen bonds C(5)—H(5)···O(1), C(16)—H(16A)···O(1), and C(20)—H(20)···O(3) together with π–π conjugation stabilized the packing of the title compound structure. Electrochemical investigation shows that there are two obvious reduction peak and that the redox process is controlled by diffusion. Furthermore, the compound was found to display good inhibition against NCI-H460 with the IC_{50} of 1.76 μmol/L. Thus, such a compound would serve as the prospective antitumor agent. The further investigation of the selectivity to cancer cell resulting in low toxicity is underway in our laboratory.

Acknowledgments

The authors are grateful to the Fundamental Research Funds for the Central Universities (lzujbky-2010-137 and lzujbky-2014-217) and Lanzhou Science and Technology Bureau Program Funds (2012-2-90) for its financial support for this project.

Appendix A. Supplementary material

Further details of the crystal structure investigations may be obtained from The Cambridge Crystallographic Data Centre via www.ccdc.cam.ac.uk/data_request/cif on quoting the depository number CCDC 995288. Supplementary data associated with this article can be found, in the online version, at http://dx.doi.org/10.1016/j.molstruc.2014.08.042. These data include MOL files and InChiKeys of the most important compounds described in this article.

References

[1] V.M. Richon, X. Zhou, R.A. Rifkind, P.A. Marks, Blood Cells. Mol. Dis. 27 (2001) 260.
[2] N.R. Ayyangar, K.C. Brahme, U.R. Kalkote, K.V. Srinivasan, Synthesis 11 (1984) 938.
[3] W. Zeng, G.Y. Zeng, S.Y. Qin, Chin. J. Org. Chem. 23 (2003) 1213.
[4] S.H. Jiang, X.D. Ma, Y.L. Xu, Chin. J. New Drugs Clin. Rem. 27 (2008) 598.
[5] R.M. Sutherland, Science 240 (1988) 177.
[6] N.V. Anil Kumar, K. Mantelingu, K.S. Rangappa, Nucleosides, Nucleotides Nucleic 21 (2002) 463.
[7] S.G. Tandon, Y.K. Agrawal, J. Chem. Eng. Data 16 (1971) 371.
[8] O.V. Dolomanov, L.J. Bourhis, R.J. Gildea, J.A.K. Howard, H. Puschmann, J. Appl. Crystallogr. 42 (2009) 339.
[9] L. Palatinus, G. Chapuis, J. Appl. Crystallogr. 40 (2007) 786.
[10] G.M. Sheldrick, in: SHELX97, Program for Crystal Structure Solutionm, University of Göttingen, Germany, 1997.
[11] G.M. Sheldrick, in: SHELXL97, Program for Crystal Structure Refinement, University of Göttingen, Germany, 1997.
[12] C.M. Liu, H.B. Cao, Y.P. Li, Y. Zhang, Adv. Mater. Res. 239 (2011) 1463.
[13] J.S. Caygill, S.D. Collyer, J.L. Holmes, F. Davis, Analyst 138 (2013) 346.
[14] Z. Ratkovic, Z.D. Juranic, T. Stanojkovic, D. Manojlovic, R.D. Vukic evic, N. Radulovic, M.D. Joksovic, Bioorg. Chem. 38 (2010) 26.
[15] N. Suzuki, T. Suzuki, Y. Ota, T. Nakano, M. Kurihara, H. Okuda, N. Miyata, J. Med. Chem. 52 (2009) 2909.
[16] S. Price, W. Bordogna, R.J. Bull, D.E. Clark, P.H. Crackett, H.J. Dyke, A.B. White, Bioorg. Med. Chem. Lett. 17 (2007) 370.